Transient anxiety and depression-like behaviors are casually associated to depletion of Forkhead box P3 expression in regulatory T cells through inflammasome activation in the brain

Giulio Pasinetti (giulio.pasinetti@mssm.edu)
Icahn School of Medicine at Mount Sinai https://orcid.org/0000-0002-1524-5196
Eun-Jeong Yang
Icahn School of Medicine at Mount Sinai

Article

Keywords: Foxp3, regulatory T cell, peripheral immune system, central immune system, inflammasome activation, depression, anxiety, transient, reversible

Posted Date: January 5th, 2023

DOI: https://doi.org/10.21203/rs.3.rs-2410197/v1

Abstract

The Forkhead box P3 (Foxp3) is a transcription factor that influences functioning of regulatory T cells (Tregs) which modulates peripheral immune response. Tregs-mediated innate and adaptive immunity are receiving considerable attention for their implication in mechanisms associated with anxiety and depression. Here, we demonstrated that depletion of Foxp3 expression causally promotes transient anxiety and depression-like behaviors associated with inflammasome activation in a Foxp3 conditional knock-out mouse. We found that restoration of Foxp3 expression causally reverses neurobehavioral changes through alteration of innate immune responses as assessed by caspase-1 activity and interleukin-1β release in the hippocampal formation of Foxp3 conditional knock-out mice. Moreover, we found that depletion of Foxp3 expression induces a significant elevation of granulocytes, monocytes, and macrophages in blood, which are associated with transient expression of the matrix metalloprotease-9, and activation of inflammasomes in the brain, as well as neurobehavioral changes. The results suggest that the dynamic regulation of Foxp3-mediated inflammatory responses may be causally associated to anxiety and depression-like behaviors through transient promotion and reversal of innate immunity in the brain. Thus, Foxp3 could be a novel therapeutic target in reversible anxiety and depression.

Introduction

Anxiety and depression are common and highly prevalent neuropsychiatric symptoms across many neurological disorders [1]. Dysregulation of functional and structural connections of the neural circuits in the hippocampal formation are reported to be a cause of anxiety and depression [2]. Recently, preclinical and clinical studies suggest the role of microglia-mediated innate immunity activation in the onset of anxiety and depression [3]. However, causality of the pro-inflammatory immune responses in the brain and related downstream pathways in anxiety and depression remain unknown.

The brain is considered an immune privileged organ, however several studies recently revealed that immune responses in the brain are influenced by peripheral immunity[4]. Peripheral immune inflammatory cascades increase permeability of the blood-brain barrier (BBB) through mechanisms involving the disruption of endothelial tight junctions or increased expression of matrix metalloproteinases (MMPs) such as MMP-9 [5, 6], leading to permeation of pro-inflammatory mediators into the brain [7]. However, the pathophysiological features of these cascades and their association with permanent or transient damages influencing neurobehavioral responses are also unknown. Thus, it is imperative to investigate whether activation of peripheral immunity may causally promote transient or permanent pathophysiological conditions in the brain for the design of novel therapeutic interventions in mood and cognitive disorders.

The transcription factor, Forkhead box P3 (Foxp3), plays a major role in the differentiation and activation of regulatory T cells (Tregs) [8]. Tregs are required for maintenance of immunological self-tolerance and immune homeostasis [9]. For example, a missense mutation in the *Foxp3* gene or depletion of Foxp3 expression impairs development and maintenance of Tregs function, leading to regulation of innate and

adaptive immunity [10, 11]. Impairments of Tregs lead to their inability to suppress inflammation in the peripheral immune system and causes autoimmune disorders including rheumatoid arthritis, systemic lupus erythematosus, and multiple sclerosis[12].

Recently, Tregs have received significant attention for their potential role in the development of anxiety and depression [13]. Evidence suggests that decreased Foxp3 expression is associated with major depressive disorders [14] and is correlated with inflammatory conditions characterized by increased levels of circulating pro-inflammatory cytokines [15]. Additionally, epigenetic regulation of *Foxp3* promoter is associated with loss of Tregs function in anxiety [16]. Interestingly, recent studies suggest efficacy of antidepressant or anxiolytic drugs through mechanisms influencing Foxp3 expression and the regulation of Tregs-associated cytokines such as interleukin (IL)-2, IL-10 and transforming growth factor-β [17]. Thus, it is possible that Foxp3 may influence anxiety and depression through mechanisms involving regulation of the peripheral immune system.

Based on this, the present study investigated the casual role of Foxp3 expression in the promotion of neurobehavioral responses associated to neuro-immune cross-talking between the peripheral and central immune systems. Using a Foxp3 conditional knock out (cKO) mouse expressing a diphtheria toxin receptor (DTR)-enhanced green fluorescent protein (GFP) transgene controlled by a *Foxp3* promoter, we found that transient depletion of Foxp3 expression causally promoted transient anxiety and depression-like behaviors possibly through mechanisms involving transient activation of inflammasomes, MMP-9 expression in the brains and dysregulation of circulating innate immune cells. We also found that depletion of Foxp3 expression in 5x Familial Alzheimer disease (FAD) mice, a mouse model of Alzheimer's disease (AD), is casually associated with AD-type cognitive impairments and neuropathological changes. This study suggests a causative role of Treg depletion in the proliferation of peripheral immune cells which concomitantly contributes to transient activation of innate immunity in the brain and causing anxiety, depression and impaired cognitive function.

Materials And Methods

Animals

All of the experimental procedures were approved by the Mount Sinai Institutional Animal Care and Use Committee (IACUC) (Approval number: IPROTO202100000013). Foxp3 cKO mice, expressing a DTR-enhanced GFP transgene controlled by a *Foxp3* promoter were purchased from Jackson Laboratories (strain: C57BL/6-Tg (Foxp3-DTR/EGFP)23.2Spar/Mmjax) and maintained by crossing C57BL/6J mice. Transgenic offspring were genotyped by PCR using the primers (Forward, F, 5'-CCCAGGTTACCATGGAGAGA-3; Reverse, R, 5'-GAACTTCAGGGTCAGCTTGC-3') and non-transgenic littermates served as age matched control. Double transgenic mice were generated by crossbreeding with Foxp3 cKO mice and 5x FAD mice which were purchased from Jackson Laboratories (strain: B6SJL-Tg [APPSwFlLon, PS1*M146L*L286V] 6799Vas/J). Double transgenic mice were identified by PCR, and non-

transgenic littermates served as age matched controls. Heterozygous of Foxp3 cKO or double heterozygous of 5xFAD/Foxp3 cKO mice were utilized for all experiments. All mice were housed on a 12 h light/dark cycle in a temperature-controlled environment.

Administration of diphtheria toxin (DT)

In order to set a protocol for administration of DT (D0564; Sigma, MO, USA), Foxp3 cKO mice were treated with 100 and 300 ng of DT or phosphate-buffered saline (PBS) to deplete Foxp3 expression without nonspecific effects. This experiment was performed independently. For other experiments, 2-month-old Foxp3 cKO mice i.p. injected every 4 days for 6 weeks with 300 ng of DT or PBS (Figure 1B). Double transgenic mice, 2-month-old 5xFAD/Foxp3 cKO mice, were treated every 4 days for 15 weeks with 300 ng of DT or PBS (Figure 6)

Behavioral tests

Behavioral tests were performed with a near-infrared camera and measured with ANY-maze™ tracking software (Stoelting, IL, USA). All animals were handled for 10 min per day for 5 days prior to experiments and were habituated to the testing room for 1 h at the beginning of the test day. All behavioral paradigms were carried out according to established protocols and described briefly below:

1) Open field test (OF): To measure total distance traveled for locomotion activity, each mouse was placed in a white box (42.5 cm L × 42.5 cm W × 42.5 cm H) and was recorded for 10 min. Total distance traveled was calculated by ANY maze software.

2) Light and dark box test (LD): To assess anxiety-like behavior, each mouse was placed in light-dark box (each compartment; 20 cm L × 40 cm W × 40 cm H) and allowed to explore the box freely. Each test was recorded for 10 min with a camera attached to the ceiling. Time spent inside the dark compartment was calculated by automated video-tracking system (ANY-maze software)

3) Forced swimming test (FST): To assess depressive-like behavior, mice were put in a transparent plastic cylinder (45 cm high and 20 cm in diameter) filled with water and each test was recorded with a digital camera for 6 min. The total duration of immobility, defined as the absence of movement in all 4 limbs, was measured using ANY-maze software.

4) Novel object recognition test (NOR): NOR was conducted as described in previous research with minor modifications[18]. During habituation, mice were placed in a white box for 10 min. The next day, mice were placed in a white box with two similar objects and were allowed to interact with the objects for 10 min. After 10 min of training, one object was replaced with a novel object and mice were placed in the box to interact with objects for 10min. To measure cognitive function, discrimination index was analyzed using ANY-maze software and was calculated as $\text{Time}_{\text{novel}}/ (\text{Time}_{\text{novel}} + \text{Time}_{\text{familiar}}) *100$.

Cells or tissue preparation

Single cell suspension samples processed for flow cytometry and cytometry by time of flight (CyTOF) were derived from mouse blood collected by retro-orbital bleeding. Each blood sample was placed in tube with EDTA and peripheral blood mononuclear cells (PBMC) were extracted by serially lysing red blood cells (RBC) in RBC lysis buffer (00-4300-54; Invitrogen, MA, USA). For tissue (spleen and brain) collection, mice from all groups were perfused after performing behavior tests. The brain tissues were separated into two hemispheres equally. One hemisphere was further dissected into the hippocampal formation and the other hemisphere was fixed with 4% paraformaldehyde (PFA) for 24 h. All samples were stored at − 80 °C or 4°C before further analysis.

Flow cytometry

Cell surface and intracellular staining were performed with monoclonal antibodies against CD3e (56-0032-82, Thermo Fisher Scientific, MA, USA), CD4 (56-0032-82, Thermo Fisher Scientific). For intracellular staining, Foxp3 Fixation/permeabilization kit (00-5523-00, Thermo Fisher Scientific) was used according to the manufacturer's instructions. Fluorescence intensities were examined as assessed by Attune NxT (Thermo Fisher Scientific) flow cytometer at the Icahn School of Medicine flow cytometry core and data were analyzed using FCS express software (CA, USA).

RNA sequencing, library preparation and analysis

Total RNA was extracted using Qiagen RNeasy Plus Mini kit (74134, Qiagen, Hilden, Germany). The RNA sequencing library was prepared using the NEBNext Ultra II RNA Library Prep Kit for Illumina (New England Biolabs, MA, USA). Samples were sequenced using a 2x150bp paired end configuration. After investigating the quality of the raw data, sequence reads were trimmed to remove possible adapter sequences and nucleotides with poor quality. The trimmed reads were mapped to the Mus musculus reference genome available on ENSEMBL. Unique gene hit counts that fell within exon regions were calculated by using feature counts from the subread package. After extraction of gene hit counts, the gene hit counts table was used for downstream differential expression analysis. Using DESeq2, a comparison of gene expression between the groups of samples was performed. The wald test was used to generate *p* values and Log2 fold changes. Significantly differentially expressed genes (DEGs) were defined by *p* values less than 0.05. For the canonical pathways, diseases/bio functions, and molecular networks analysis of DEGs, we used the commercial QIAGEN Ingenuity® Pathway Analysis (IPA, QIAGEN) software. For the canonical pathways, diseases/bio functions and comparison analysis, −log (*p* value) > 1.3 was taken as the threshold, a Z score > 2 was defined as the threshold of activation, and a Z score < -2 was defined as the threshold of inhibition. The score of molecular networks analysis was calculated by IPA.

Western blotting

Extracted protein samples from hippocampal formation (45 µg) were separated by electrophoresis on 4% to 15% sodium dodecyl sulfate-polyacrylamide gels and transferred to a nitrocellulose membrane. The membranes were then blocked for 1 hour at room temperature (RT), followed by overnight treatment with

primary antibodies (anti-caspase-1 antibody, 20B-0042; anti-IL-1β antibody 6243S; anti-α-tubulin antibody, T9026) at 4°C. The next day, the blots were treated with a secondary antibody conjugated with horseradish peroxidase (anti-rabbit-or anti-mouse IgG -HRP-antibodies) for 1h at RT. The bands were detected using chemiluminescence detection kit (32106; Thermo Fisher Scientific) and data was analyzed using image J software to measure relative protein expression.

RNA extraction and Real-Time Quantitative Reverse Transcription PCR (RT-qPCR)

Total RNA from brain, spleen, and PBMC were extracted using Quick RNA extraction Kit (Zymo research, CA, USA). Strand cDNA was synthesized from 100 ng of total RNA using High-Capacity cDNA Reverse Transcription Kit (4368814, Applied Biosystems, MA, USA) as per the manufacturer's instructions. RT-qPCR was performed by the Icahn School of Medicine qPCR Core and analyzed by ABI PRISM 7900HT Sequence Detection System (Applied Biosystems). Utilized cycling conditions were as follows: 95 °C for 2 min, followed by 40 cycles of 95 °C for 15 s, 60 °C for 15 s, and 72 °C for 1 min. The primer sequences were as follows: *Foxp3*-F, 5'-AGAGCTCTTGTCCATTGAGGCCA-3', *Foxp3*-R, 5'-TGTCCTGGGCTACCCTACTG-3'; *Cxcl10*-F, 5'-ATGACGGGCCAGTGAGAATG-3', *Cxcl10*-R, 5'-GAGGCTCTCTGCTGTCCATC-3'; *Caspase-1*-F, 5'- CACATTTCCAGGACTGACTGG-3', *Caspase-1*-R, 5'-AGACGTGTACGAGTGGTTGT-3'; *Nlrp3-F*, 5'-AGAAGAGACCACGGCAGAA-3', *Nlrp3*-R, 5'-CCTTGGACCAGGTTCAGTGT -3', *IL-1β*-F, 5'-TTCAGGCAGGCAGTATCACTC-3'; *IL-1β*-R, 5'-CCACGGGAAAGACACAGGTAG-3'; *Hprt-F,* 5'-CCCCAAAATGGTTAAGGTTGC-3', *Hprt-R*-5'-AACAAAGTCTGGCCTGTATCC-3. Expression level of *Hprt* was used as an internal control and relative mRNA expression of other genes were quantified using the $2^{-\Delta\Delta Cq}$ method.

CyTOF and data analysis

All samples were processed by the Mount Sinai Human Immune Monitoring Center and CyTOF was conducted as described in previous research [19]. Normalized data files were analyzed using FCS express software for manual cleaning and gating different immune cells to create 2 and high dimensional (t-distributed stochastic neighbor embedding, t-SNE) plots. t-SNE clustering was performed on 16 parameters where equal event sampling was selected in PBMC. t-SNE analysis was performed using equal sampling per comparison, perplexity=80, iterations=1,000.

Cytokine array

Proteome Profiler Array (ARY006; R&D System, MN, USA) was used to measure cytokines, chemokines and acute phase protein as described previously [20]. Briefly, 100 µl of plasma samples in blocking buffer were incubated to membranes containing antibody arrays overnight as at 4°C on a shaker. The membranes were incubated with the biotinylated antibody cocktail solution and horseradish peroxidase-conjugated streptavidin for 3 or 2 hours at RT, respectively. All membrane were developed with the detection reagent provided by the manufacturer and were scanned to obtain images for analysis of pixel densities using the Image J software. Positive controls were used for normalization and mean values were calculated.

Enzyme-linked immunosorbent assays (ELISAs)

ELISAs were performed using mouse β-amyloid beta40 (Aβ40, KMB3481; Invitrogen) and mouse Aβ42 (KMB3441; Invitrogen) ELISA kits to determine the amount of $A\beta_{1\text{-}40}$ and $A\beta_{1\text{-}42}$ following the manufacturer's instructions. Briefly, frozen brain tissue were homogenized in a cold buffer, which consisted of 5 M guanidine-HCl/50 mM Tris supplemented with inhibitor cocktail containing AEBSF (78431; Thermo Fisher Scientific) and then incubated with an orbital shaker for 3 h at RT. 100 µl of standards and sample, which were diluted with standard diluent buffer, were applied to Aβ40 or Aβ42 polyclonal antibody-precoated 96-well plates. The plates were read at 450 nm using a microplate reader (VarioskanTM Lux; Thermo Fisher Scientific). Concentrations of $A\beta_{1\text{-}40}$ and $A\beta_{1\text{-}42}$ were calculated using the standard curves and both were normalized by total amount of protein from each sample using the BCA assay (23225; Thermo Fisher Scientific).

Immunohistochemistry

Brains were cut into 50 µm coronal sections and sections were washed in PBS and incubated in blocking solution (10% normal goat serum, 0.1% Triton X-100) for 1h at RT. Sections were then incubated with primary antibody in blocking solution overnight at 4°C. 6E10 (SIG39320, Biolegend, CA, USA) was used as a primary antibody. After the primary immunoreaction, sections were incubated with Alexa 488 (A11001, Invitrogen) conjugated secondary antibodies. LSM 800 confocal microscope (Carl Zeiss, Jena, Germany) was used for visualization of immunostaining of the sections.

Statistical analysis

All data are expressed as the mean ± standard error of the mean. Data were calculated using a t-test and one or two-way analysis of variance (ANOVA) followed by Tukey's post hoc analysis (*$p < 0.05$, **$p < 0.01$, ***$p<0.001$). All statistical analyses were performed using GraphPad Prism 8 software (GraphPad Software Inc., San Diego, CA, USA).

Results

Dynamical regulation of Foxp3 depletion is mediated by DT treatment in Foxp3 cKO mice.

Here, we investigated the regional distribution of mRNA expression of *Foxp3* in the PBMC, spleen, and brain to estimate abundance of Foxp3 expression using Foxp3 cKO mice. As shown in Fig. 1A, *Foxp3* mRNA expression in PBMC and spleen were approximately two order of magnitude higher compared to the expression in the brain (*$p < 0.05$).

We utilized a Foxp3 cKO mice, expressing DTR-eGFP transgene under control of *Foxp3* promoter allowing depletion of Foxp3 expression by DT treatment to transiently deplete Foxp3 expression (Fig. 1B). After treatment of DT with different concentrations (100 ng and 300 ng) for 6 weeks, we observed a dose-dependent decrease of Foxp3-dependent GFP expression compared to the vehicle treated group (*$p <$

0.05, Fig. 1C). Based on titration of study, we selected the dose of 300ng of DT to deplete Foxp3 expression for subsequent experiments (Fig. 1B). We next examined whether DT treatment induces depletion of Foxp3 expression in the brain, spleen, and PBMC of Foxp3-depleted mice (Fig. 1D-F). We found no difference in *Foxp3* mRNA expression in the brain of Foxp3-depleted mice compared to age matched control mice (Fig. 1D). However, *Foxp3* mRNA expression was significantly decreased by 46% in spleen of Foxp3-depleted mice compared to age matched control (*$p < 0.05$, Fig. 1E).

We also observed that Foxp3-dependant GFP expression was significantly reduced by approximately 60% in PBMC of Foxp3-depleted mice (*$p < 0.05$, Fig. 1F). Moreover, reduction of Foxp3-dependant GFP expression in PBMC returned to baseline level in Foxp3-restored mice following withdrawal of DT for 8 weeks as assessed by flow cytometry (Fig. 1G).

Taken together, these results indicate that administration of DT in Foxp3 cKO mice induced transient depletion of Foxp3 expression selectively in PBMC after treatment with 300 ng of DT for 6 weeks and its expression was restored to the baseline level following withdrawal of DT.

Transient depletion of Foxp3 expression in PBMC is causally associated to promotion of anxiety or depression-like behaviors in Foxp3 cKO mice.

To investigate causal association between peripheral Foxp3 expression and anxiety/depression-like behaviors in Foxp3 ckO mice, we performed LD, FST and OF to assess locomotion activity, anxiety and depression-like behavior, respectively. No significant change was observed in body weight between treatment with DT and vehicle in Foxp3 cKO mice for treatment period (Fig. 1B and Fig. 2A). Changes in locomotor activity after depletion or restoration of Foxp3 expression in Foxp3 cKO mice was assessed by total distance traveled; no change between Foxp3-depleted, Foxp3-restored mice, and age matched control mice was found (Fig. 2D). These control studies suggest that DT-mediated depletion of Foxp3 expression for 6 weeks was well tolerated in Foxp3 cKO mice at 300ng regimen.

In the LD, Foxp3-depleted mice spent significantly more time in dark area after depletion of Foxp3 expression (***$p < 0.001$, Fig. 2B, left panel). In addition, we also observed that Foxp3-depleted mice also exhibited increased immobility time in FST after depletion of Foxp3 expression (**$p < 0.01$, Fig. 2C, left panel). Interestingly, these neurobehavioral impairments were ameliorated after restoration of Foxp3 expression in Foxp3-restored mice compared to age matched control mice (Fig. 2B and 2C, right panels). In particular, we find that Foxp3 expression in PBMC were negatively correlated with anxiety (*$p < 0.05$, Fig. 2E) and depression-like behavior (*$p < 0.05$, Fig. 2F).

These results support that transient depletion of Foxp3 expression in PBMC may casually influence anxiety or depression-like behaviors.

Transient Foxp3 depletion is causally associated to differentially expressed genes (DEGs) related with inflammatory response and immune cells trafficking in the hippocampal formation of Foxp3-depleted mice

To understand a potential molecular mechanism of the association between peripheral Foxp3 expression and neurobehavioral changes, RNA sequencing was performed in the hippocampal formation of Foxp3-depleted and Foxp3-restored mice. Hippocampal formation is one of crucial brain regions strongly involved in anxiety and depression-like behaviors in rodents [2].

As shown Fig. 3A, a total of 17,237 genes DEGs were identified in a volcano plot (Fig. 3A, upper panel) and among these genes, 401 DEGs were up-regulated and 422 DEGs were down-regulated significantly in Foxp3-depleted mice compared to age matched control mice (*$p < 0.05$, Fig. 3A, bottom panel). To explore the involvement of 823 annotated DEGs in canonical pathways and diseases/bio functions, functional prediction analysis was performed according to IPA software (Fig. 3B and Fig. 3C). For canonical pathways analysis, a total of 7 enriched canonical pathways were identified by applying absolute z scores greater than 2 and statistical significance (*$p < 0.05$). The top 3 canonical pathways, '*Role of hypercytokinemia /hyperchemokinemia in the pathogenesis of influenza*', '*Role of pattern recognition receptors in recognition of bacteria and viruses*' and '*Interferon signaling*' were identified among 7 other canonical pathways (Fig. 3B, left panel). We also found the expression of 13 DEGs in the top 3 canonical pathways where significantly altered in Foxp3-depleted mice compared to age matched control mice (Fig. 3B, right panel). In addition, diseases and bio functions analysis, by applying absolute z scores greater than 2 and statistical significance, revealed activation of functional categories related to '*Cell-mediated immune response'* and *'Immune cells trafficking'* in Foxp3-depleted mice (Fig. 3C).

To investigate whether identified canonical pathways and diseases/bio functions in Foxp3-depleted mice were transiently regulated in Foxp3-restored mice as found in neurobehavioral changes, a comparison analysis was performed by IPA applying absolute z scores greater than 2 and statistical significance (Fig. 3D and 3E). As shown in Fig. 3D, we found the top 9 canonical pathways being enriched in Foxp3-depleted mice were recovered in Foxp3-restored mice. Among these 9 canonical pathways, 5 of them are associated to inflammatory response such as '*Role of hypercytokinemia/ hyperchemokinemia in the pathogenesis of influenza', 'Role of pattern recognition receptors in recognition of bacteria and viruses', 'Interferon signaling', 'Role of OKR in interferon induction and antiviral response' and 'Neuroinflammation signaling'* (Fig. 3D). Moreover, significant activated cellular function, which were related to '*Innate immune response', and 'Immune cells movement'* were observed in Foxp3-depleted mice and these changes were significantly mitigated in Foxp3-restored mice (Fig. 3E).

Taken together, our results suggest that transient depletion of Foxp3 expression promote inflammatory responses such as immune cell trafficking and inflammasome activation in the hippocampal formation which causally coincided with the transient anxiety and depression-like behaviors.

Transient depletion of Foxp3 expression results in elevated Cxcl10 **expression and inflammasome activation in Foxp3 cKO mice.**

In a validation study of the transcriptomic investigation and IPA analysis, we assessed mRNA expression of four candidate genes, which are associated with inflammatory responses, in the hippocampal

formation of Foxp3-depleted and Foxp3-restored mice as assessed by RT-qPCR. We found that mRNA expression of *Cxcl10* (Fig. 4A), a chemokine that plays a key role in controlling leukocyte trafficking into brain, was significantly elevated in the Foxp3-depleted mice compared to age matched control mice (**$p < 0.01$, Fig. 4A, left panel), while no significant difference in *Cxcl10* mRNA expression was identified in Foxp3-restored mice compared to age matched control mice (Fig. 4A, right panel). We also measured mRNA expression of *Nlrp3*, *Caspase-1* and *IL-1β* to confirm inflammasome activation in the hippocampal formation of Foxp3-depleted mice and Foxp3-restored mice (Fig. 4B-D). The levels of *Nlrp3*, *Caspase-1* and *IL-1β* mRNA were significantly increased 2, 1.4, and 1.3-fold in Foxp3-depleted mice, respectively (*$p < 0.05$, **$p < 0.01$, Fig. 4B-D, left panels). Interestingly, no differences in Foxp3-restored mice was found compared to age matched control mice (Fig. 4B-D, right panels).

In a further confirmatory study, the protein expression of Pro-caspase-1, Caspase-1 and IL-1β and inflammasome activation markers were assessed by gel-blot assay (western blotting, Fig. 4E-4H). As shown in Fig. 4E, we confirmed that cleaved Caspase-1 expression (Fig. 4E) and IL-1β expression (Fig. 4F) were significantly increased in Foxp3-depleted mice compared to those of expression in age matched control mice (*$p < 0.05$, **$p < 0.01$, Fig. 4E and 4F). Interestingly, non-detectable changes in Pro-caspase-1, Caspase-1 (Fig. 4G) and IL-1β (Fig. 4H) in the Foxp3-restored mice compared to the age matched control mice were observed.

Overall, these results support the hypothesis that transient depletion of Foxp3 expression may casually and transiently influence brain innate immunity changes which coincided with transient anxiety and depression-like behaviors.

Depletion of Foxp3 expression increases the number of peripheral innate immune cells coincidentally with transient increase of MMP-9 expression in the brain of Foxp3 cKO mice.

Foxp3 is a specific marker of Treg cells influencing immune tolerance through suppression of immune responses [9]. Moreover, Treg cells may also promote innate and adaptive immunity [21, 22]. We hypothesized that depletion of Foxp3 expression may modulate innate or adaptive immune cell populations in PBMC. Using CyTOF analysis, we assessed the immune profiles of PBMC in Foxp3-depleted mice compared to age matched control mice. To visualize clustering of each cell types, t-SNE analysis was performed based on gate strategy (Fig. 5A and Fig. 5C). All CyTOF were pre-processed and living single immune cells ($CD45^+$) were retained after gating for further analysis (Fig. 5C). Each immune cell coordinates according to their expression of the 6 measure parameters including CD3e, CD4, CD8, CD11, CD19 and Ly-6G (Fig. 5A and C). As shown in Fig. 5B, we identified 5 major immune cell populations, including B lymphocytes ($CD3e^-CD19^+$), $CD4^+$ T lymphocytes ($CD3e^+CD4^+$), $CD8^+$ T lymphocytes ($CD3e^+CD8^+$), macrophages/monocytes ($CD3^-CD19^-CD11b^+LY\text{-}6G^-$) and granulocytes ($CD3^-CD19^-CD11b^+LY\text{-}6G^+$) based on the canonical cell markers. The t-SNE analysis revealed that depletion of Foxp3 expression increased the proportion of granulocytes or macrophages/monocytes, while other subtypes of immune cells (B lymphocytes, T lymphocytes) showed a similar pattern in Foxp3-depleted mice compared to age matched control (Fig. 5B). Next, we quantified the sub-population of each immune cell type in Foxp3-

depleted mice compared to age matched control (Fig. 5D-5F). There were no significant differences between Foxp3-depleted mice and age matched control mice in respect with the percentage of $CD3e^{-}CD19^{+}$cells, $CD3e^{+}CD19^{-}$ cells, $CD3e^{+}CD4^{+}$ cells and $CD3e^{+}CD8^{+}$ cells (Fig. 5E and 5F). Interestingly, the percentage of $CD3^{-}CD19^{-}CD11b^{+}LY\text{-}6G^{+}$ cells (granulocytes, Fig. 5D, left panel) and $CD3^{-}CD19^{-}CD11b^{+}LY\text{-}6G^{-}$ cells (macrophages/monocytes, Fig. 5D, right panel) were significantly higher by 84% and 23%, respectively compared to age matched control mice (*$p < 0.05$, Fig. 5D).

Based on this evidence suggesting a role of Tregs in the regulation of innate immune cells, next we explored alteration of cytokines or chemokine production released by innate immune cells in plasma of Foxp3-depleted mice using a proteome profiler array. A total of 6 cytokines were altered in Foxp3-depleted mice with significantly 4 cytokines upregulated (interferon-gamma, IFN-γ; macrophage-colony stimulating factor, M-CSF; triggering receptor expressed on myeloid cells-1, TREM-1; IL-13), 1 cytokine downregulated (tissue inhibitor of metallopeptidase-1, TIMP-1) and a tendency toward 1 cytokine upregulated (IL-17) compared to age matched control mice (Fig. 5G). These results suggest the potential alteration of peripheral innate immunity through depletion of Foxp3 expression.

Several studies have reported that granulocytes derived MMP-9 activity may lead to damage of the BBB[23]. Based on this evidence and our immune profiling outcome showing elevated levels of granulocyte and monocytes/macrophages, we continued to explore MMP-9 expression in the brain. As shown in Fig. 5H, Foxp3-depleted mice showed significant transient elevation of MMP-9 expression in the hippocampal formation (*$p < 0.05$, Fig. 5H) compared to age matched control mice which we found being restored to baseline level in Foxp3-restored mice (Fig. 5I). These results suggest that depletion of Foxp3 expression in PBMC may lead to an increase of innate immune cells, possibly influencing transient MMP-9 expression in the brain.

Depletion of Foxp3 expression induces inflammasome activation coinciding with cognitive impairment and Aβ peptide burden in the hippocampal formation in the 5XFAD mice.

Further IPA-derived functional network mapping analysis was performed to identify direct and indirect relationships among DEGs and DEGs' regulators in Foxp3-depleted mice, which suggested the '*Developmental disorder, hereditary disorder, and metabolic disease*' network being highly predicated among 31 molecules (score 48). Among them, we found amyloid precursor protein (APP) which is associated with pathogenesis of AD being predicted as a key molecule in Foxp3-depleted mice (Fig. 6A). To examine the relevance of this mechanism in AD pathogenesis, we generated a double transgenic 5xFAD/Foxp3 cKO mouse model to investigate whether depletion of Foxp3 expression in 5xFAD mice would accelerate cognitive impairment and AD neuropathology compared to 5xFAD mice as assessed by NOR (Fig. 6B, upper panel). In a control study, we found no significant change of locomotion activity between all experimental mice groups (Fig. 6B, bottom panel). Interestingly, discrimination index as a measure of memory function significantly decreased in 5.5-month-old 5xFAD/Foxp3-depleted mice which are pre-symptomatic at this age. (*$p < 0.05$, Fig. 6B, bottom panel). We next evaluated the levels of Aβ peptide and Aβ burden, the hallmark neuropathological characteristic of AD, assessed by ELISA and

immunohistochemistry, respectively. We find that statistical significance for reduction of $A\beta_{1-40}$ isoform and increase of $A\beta_{1-42}$ isoform, with resulting increase of $A\beta_{1-42}$ / $A\beta_{1-40}$ ratio in hippocampal formation of 5xFAD/Foxp3-depleted mice (*$p < 0.05$, Fig. 6C). In addition, elevation of Aβ plaque burden was observed in dentate gyrus layer of hippocampal formation in 5xFAD/Foxp3-depleted mice compared to age matched 5xFAD mice as assessed by 6E10 immunostaining (Fig. 6D).

This evidence was of high interests in view of the fact that inflammasome activation is currently implicated in mechanisms associated with Aβ pathology and neurodegeneration [24, 25]. Based on this, we next examined the potential role of caspase-1 activation and IL-1β generation in 5xFAD/Foxp3-depleted mice (Fig. 6E and 6F). We found the protein expression of the active form of Caspase-1 in the hippocampal formation was significantly increased in 5xFAD/Foxp3-depleted mice compared to age matched 5xFAD mice (*$p < 0.05$, Fig. 6E). In addition, 5xFAD/Foxp3-depleted mice showed an increasing trend of elevation of IL-1β compared to age matched 5xFAD mice ($p = 0.0611$, Fig. 6E).

Taken together, these results demonstrate that depletion of Foxp3 expression may lead to inflammasome activation, AD-type neuropathology, and acceleration of the onset of cognitive impairment.

Discussion

In this study, we elucidate the potential role of Foxp3, a transcription factor of Tregs, in the mechanism associated with neurobehavioral changes including anxiety and depression-like behaviors using Foxp3 cKO mice. Our study revealed that Foxp3 is a novel key factor in anxiety and depression-like behaviors through dynamic regulation of inflammatory responses including increased in the number of innate immune cells in PBMC, BBB disruption, and inflammasome activation in brain. Interestingly, all were restored into baseline level concomitantly with neurobehavioral recovery following restoration of Foxp3 expression in Foxp3 cKO mice.

Impaired function of Tregs has been implicated in the development of anxiety and depression [14, 15, 26, 27], and antidepressant/anxiolytic treatment are improved by increasing the number of Tregs and improving their function [28, 29]. Our data demonstrate that transient anxiety and depression-like behaviors were observed in Foxp3 cKO mice, followed by DT treatment and then withdrawal of DT treatment to induce acute inflammation mediated by Foxp3 depletion and to return to its normal state through Foxp3 restoration, respectively. Our results are consistent with other studies that reported a potential relationship between Foxp3 and the development of anxiety and depression-like behaviors. Interestingly, we found that both anxiety and depression-like behaviors were significantly modulated dependent on Foxp3 expression in PBMC (Fig. 2). Despite a distinct association between Foxp3 and anxiety/depression-like behaviors, a detailed mechanism for peripheral and central immune communication in anxiety and depression has not yet been investigated.

Several research studies have implicated the role of inflammasome activation in anxiety and depression [30, 31]. A study reported that a chronic stress mouse model showed elevated NLRP3 inflammasome

activation and IL-1β level in hippocampal formation associated with anhedonia and depression like behavior [30]. Inhibition of inflammasome activation in this model blocked depression-like behavior with reduced IL-1β production [30]. In addition, mice lacking NLRP3 were resistant to anxiety-like behavior and blockade of inflammasome activation signaling using P2X7 antagonist attenuated anxiety-like behavior [32, 33]. Our results show that Foxp3-depleted mice showed inflammasome activation including increased cleavage of Caspase-1 and IL-1β production in hippocampal formation. Interestingly, we found that restoration of Foxp3 expression ameliorated cleavage of Caspase-1 and IL-1β production in hippocampal formation concomitantly to neurobehavioral recovery (Figs. 3 and 4).

It is known that pro-inflammatory cytokines including IL-1β, as well as IL-6 and tumor necrosis factor-α controlled by inflammasome is integrated in anxiety and depression [34], however it is still not been identified how inflammasome in brain is activated. To examine the pathways and mechanisms underlying inflammasome activation, we hypothesized that activation of peripheral immune cells-mediated by depletion of Foxp3 expression may promote inflammasome activation through increased infiltration of innate immune cells into the brain. Our data demonstrate that the number of circulating innate immune cells including granulocytes are elevated, and increased expression of pro-inflammatory cytokines including IFN-γ, M-CSF, TREM-1 and IL-17 released from innate immune cells in Foxp3-depleted mice (Fig. 5). In addition, our data show elevated expression of MMP-9 released by granulocytes, diminished TIMP-1 expression, a tissue inhibitor of metalloproteinase and increased expression of *Cxcl10* secreted by activated innate immune cells (Fig. 4–5). We also identified that the biological process associated DEGs in Foxp3-depleted mice is *'Immune cell trafficking'* through IPA functional analysis (Fig. 3). Taken all together, our study suggests that activation of innate immune cells may bridge the gap between inflammasome activation in brain and transient of Foxp3 expression in PBMC, which is a key factor in the pathogenesis of anxiety and depression-like behaviors.

In this study, we investigated that depletion of Foxp3 expression causally promotes transient anxiety and depression-like behaviors, associated with immune system plasticity using Foxp3 cKO mice followed by DT treatment. To exclude the effects of DT on neurobehavioral changes and immune response, we also performed behavior tests and biochemical experiments using WT mice followed by vehicle and DT treatment. There were no significant changes of body weight, neurobehavioral changes, and inflammasome activation in the brain (supplemental Fig. 1). In addition, our study supports that pharmacological intervention promoting Foxp3 expression in PBMC may causally attenuate acute forms of anxiety and depression-like behaviors coincidentally with restoration of potentially innate immune mediated cascades in the brain. We hypothesize that chronic inflammatory responses-mediated by Foxp3 depletion eventually cause irreversible neurological damages including BBB disruption and a permissive pro-inflammatory state, leading to chronic inflammation in the brain explaining certain forms of untreatable anxiety and depression condition. Further studies are needed to investigate the potential role of chronic depletion of Foxp3 expression in anxiety and depression-like behaviors associated with risk of irreversible brain degeneration including permeant BBB damage.

Depression and anxiety are observed in AD patients with cognitive decline [35]. The prevalence of anxiety ranges from 9.4–39% and the prevalence of depression ranges from 14.8–40% in various stages of AD [36]. In addition, recent studies revealed a significant strong relationship between anxiety, depression, cognitive decline and neuropathology of AD [37]. Similarly, we found that depletion of Foxp3 expression induced inflammasome activation, influencing AD-like neuropathological changes and exacerbating cognitive impairment at a pre-symptomatic stage in 5xFAD mice (Fig. 6). Inflammasome activation has been associated with the progression of AD [38]. However, it is still unknown how inflammasome is activated in the early stage of AD. Based on our study, Foxp3-driven inflammasome pathway may play an important role in the onset and progression of AD. Further in-depth studies are needed to validate potential mechanisms related to innate and adaptive immunity alteration in peripheral and central immune system to elucidate specific biological mechanisms-mediated by Foxp3 expression in AD.

Collectively, out study supports that Foxp3 may causally influence peripheral immune response which induce transient pro-inflammatory cascade in brain, leading to anxiety, depression-like behaviors and cognitive decline.

Declarations

Author Contributions

E. Yang conceived and designed the study concept, performed all experiments, analyzed and interpreted data, and was instrumental in the writing of the manuscript. G.M.P. conceived and designed the study concept, and supervised the project. In addition, G.M.P. is the guarantor of this work, as such; he has full access to all the data in the study and takes responsibility for the integrity of the data and the accuracy of the data analysis. All authors read the final version of the manuscript, revised it critically, and gave final approval of the version submitted.

Acknowledgments

G.M.P. holds a Senior VA Career Scientist Award. We acknowledge that the contents of this study do not represent the views of the NCCIH, the ODS, the National Institutes of Health, the U.S. Department of Veterans Affairs, or the United States Government. The authors would also like to thank Md Al Rahim for his technical assistance, and Joshua Palmieri for his impeccable work with administrative duties.

Funding and additional information

This research was supported by a grant (AT008661) from the NIG's Office of Dietary Supplements (ODS) and the National Center for Complementary and Integrative Health, awarded to G.M.P. The study was supported by the generous support of the Altschul Foundation to G.M.P.

Declaration of Interests

The authors have no conflict of interest to report.

Data Availability

The authors declare that the data supporting the findings of this study are available within the paper and its Supplementary Information files. Any remaining data that support the results of the study will be available from the corresponding author upon reasonable request.

References

1. Gold SM, Kohler-Forsberg O, Moss-Morris R, Mehnert A, Miranda JJ, Bullinger M *et al.* Comorbid depression in medical diseases. *Nat Rev Dis Primers* 2020; **6**(1)**:** 69.
2. Duman RS, Aghajanian GK, Sanacora G, Krystal JH. Synaptic plasticity and depression: new insights from stress and rapid-acting antidepressants. *Nat Med* 2016; **22**(3)**:** 238-249.
3. Afridi R, Suk K. Neuroinflammatory Basis of Depression: Learning From Experimental Models. *Front Cell Neurosci* 2021; **15:** 691067.
4. Engelhardt B, Vajkoczy P, Weller RO. The movers and shapers in immune privilege of the CNS. *Nat Immunol* 2017; **18**(2)**:** 123-131.
5. Luissint AC, Artus C, Glacial F, Ganeshamoorthy K, Couraud PO. Tight junctions at the blood brain barrier: physiological architecture and disease-associated dysregulation. *Fluids Barriers CNS* 2012; **9**(1)**:** 23.
6. Prinz M, Priller J. The role of peripheral immune cells in the CNS in steady state and disease. *Nat Neurosci* 2017; **20**(2)**:** 136-144.
7. Sun Y, Koyama Y, Shimada S. Inflammation From Peripheral Organs to the Brain: How Does Systemic Inflammation Cause Neuroinflammation? *Front Aging Neurosci* 2022; **14:** 903455.
8. Lee W, Lee GR. Transcriptional regulation and development of regulatory T cells. *Exp Mol Med* 2018; **50**(3)**:** e456.
9. Ramsdell F, Ziegler SF. FOXP3 and scurfy: how it all began. *Nat Rev Immunol* 2014; **14**(5)**:** 343-349.
10. Hayatsu N, Miyao T, Tachibana M, Murakami R, Kimura A, Kato T *et al.* Analyses of a Mutant Foxp3 Allele Reveal BATF as a Critical Transcription Factor in the Differentiation and Accumulation of Tissue Regulatory T Cells. *Immunity* 2017; **47**(2)**:** 268-283 e269.
11. Lucca LE, Dominguez-Villar M. Modulation of regulatory T cell function and stability by co-inhibitory receptors. *Nat Rev Immunol* 2020; **20**(11)**:** 680-693.
12. Dominguez-Villar M, Hafler DA. Regulatory T cells in autoimmune disease. *Nat Immunol* 2018; **19**(7)**:** 665-673.
13. Miller AH, Raison CL. The role of inflammation in depression: from evolutionary imperative to modern treatment target. *Nat Rev Immunol* 2016; **16**(1)**:** 22-34.
14. Grosse L, Hoogenboezem T, Ambree O, Bellingrath S, Jorgens S, de Wit HJ *et al.* Deficiencies of the T and natural killer cell system in major depressive disorder: T regulatory cell defects are associated with inflammatory monocyte activation. *Brain Behav Immun* 2016; **54:** 38-44.

15. Toben C, Baune BT. An Act of Balance Between Adaptive and Maladaptive Immunity in Depression: a Role for T Lymphocytes. *J Neuroimmune Pharmacol* 2015; **10**(4)**:** 595-609.
16. Prelog M, Hilligardt D, Schmidt CA, Przybylski GK, Leierer J, Almanzar G *et al.* Hypermethylation of FOXP3 Promoter and Premature Aging of the Immune System in Female Patients with Panic Disorder? *PLoS One* 2016; **11**(6)**:** e0157930.
17. Jahangard L, Behzad M. Diminished functional properties of T regulatory cells in major depressive disorder: The influence of selective serotonin reuptake inhibitor. *J Neuroimmunol* 2020; **344:** 577250.
18. Leger M, Quiedeville A, Bouet V, Haelewyn B, Boulouard M, Schumann-Bard P *et al.* Object recognition test in mice. *Nat Protoc* 2013; **8**(12)**:** 2531-2537.
19. Westfall S, Caracci F, Estill M, Frolinger T, Shen L, Pasinetti GM. Chronic Stress-Induced Depression and Anxiety Priming Modulated by Gut-Brain-Axis Immunity. *Front Immunol* 2021; **12:** 670500.
20. Yang EJ, Kim H, Choi Y, Kim HJ, Kim JH, Yoon J *et al.* Modulation of Neuroinflammation by Low-Dose Radiation Therapy in an Animal Model of Alzheimer's Disease. *Int J Radiat Oncol Biol Phys* 2021; **111**(3)**:** 658-670.
21. Okeke EB, Uzonna JE. The Pivotal Role of Regulatory T Cells in the Regulation of Innate Immune Cells. *Front Immunol* 2019; **10:** 680.
22. Romano M, Fanelli G, Albany CJ, Giganti G, Lombardi G. Past, Present, and Future of Regulatory T Cell Therapy in Transplantation and Autoimmunity. *Front Immunol* 2019; **10:** 43.
23. Galea I. The blood-brain barrier in systemic infection and inflammation. *Cell Mol Immunol* 2021; **18**(11)**:** 2489-2501.
24. Heneka MT, Kummer MP, Stutz A, Delekate A, Schwartz S, Vieira-Saecker A *et al.* NLRP3 is activated in Alzheimer's disease and contributes to pathology in APP/PS1 mice. *Nature* 2013; **493**(7434)**:** 674-678.
25. Ising C, Venegas C, Zhang S, Scheiblich H, Schmidt SV, Vieira-Saecker A *et al.* NLRP3 inflammasome activation drives tau pathology. *Nature* 2019; **575**(7784)**:** 669-673.
26. Grosse L, Carvalho LA, Birkenhager TK, Hoogendijk WJ, Kushner SA, Drexhage HA *et al.* Circulating cytotoxic T cells and natural killer cells as potential predictors for antidepressant response in melancholic depression. Restoration of T regulatory cell populations after antidepressant therapy. *Psychopharmacology (Berl)* 2016; **233**(9)**:** 1679-1688.
27. Chen Y, Jiang T, Chen P, Ouyang J, Xu G, Zeng Z *et al.* Emerging tendency towards autoimmune process in major depressive patients: a novel insight from Th17 cells. *Psychiatry Res* 2011; **188**(2)**:** 224-230.
28. Schneider-Schaulies J, Beyersdorf N. CD4+ Foxp3+ regulatory T cell-mediated immunomodulation by anti-depressants inhibiting acid sphingomyelinase. *Biol Chem* 2018; **399**(10)**:** 1175-1182.
29. Singh A, Dashnyam M, Chim B, Escobar TM, Dulcey AE, Hu X *et al.* Anxiolytic Drug FGIN-1-27 Ameliorates Autoimmunity by Metabolic Reprogramming of Pathogenic Th17 Cells. *Sci Rep* 2020; **10**(1)**:** 3766.

30. Zhang Y, Liu L, Liu YZ, Shen XL, Wu TY, Zhang T *et al.* NLRP3 Inflammasome Mediates Chronic Mild Stress-Induced Depression in Mice via Neuroinflammation. *Int J Neuropsychopharmacol* 2015; **18**(8).
31. Alcocer-Gomez E, de Miguel M, Casas-Barquero N, Nunez-Vasco J, Sanchez-Alcazar JA, Fernandez-Rodriguez A *et al.* NLRP3 inflammasome is activated in mononuclear blood cells from patients with major depressive disorder. *Brain Behav Immun* 2014; **36:** 111-117.
32. Alcocer-Gomez E, Ulecia-Moron C, Marin-Aguilar F, Rybkina T, Casas-Barquero N, Ruiz-Cabello J *et al.* Stress-Induced Depressive Behaviors Require a Functional NLRP3 Inflammasome. *Mol Neurobiol* 2016; **53**(7)**:** 4874-4882.
33. Iwata M, Ota KT, Li XY, Sakaue F, Li N, Dutheil S *et al.* Psychological Stress Activates the Inflammasome via Release of Adenosine Triphosphate and Stimulation of the Purinergic Type 2X7 Receptor. *Biol Psychiatry* 2016; **80**(1)**:** 12-22.
34. Iwata M, Ota KT, Duman RS. The inflammasome: pathways linking psychological stress, depression, and systemic illnesses. *Brain Behav Immun* 2013; **31:** 105-114.
35. Lyketsos CG, Lopez O, Jones B, Fitzpatrick AL, Breitner J, DeKosky S. Prevalence of neuropsychiatric symptoms in dementia and mild cognitive impairment: results from the cardiovascular health study. *JAMA* 2002; **288**(12)**:** 1475-1483.
36. Ma L. Depression, Anxiety, and Apathy in Mild Cognitive Impairment: Current Perspectives. *Front Aging Neurosci* 2020; **12:** 9.
37. Pink A, Krell-Roesch J, Syrjanen JA, Vassilaki M, Lowe VJ, Vemuri P *et al.* A longitudinal investigation of Abeta, anxiety, depression, and mild cognitive impairment. *Alzheimers Dement* 2022; **18**(10)**:** 1824-1831.
38. Zhang Y, Dong Z, Song W. NLRP3 inflammasome as a novel therapeutic target for Alzheimer's disease. *Signal Transduct Target Ther* 2020; **5**(1)**:** 37.

Figures

Figure 1

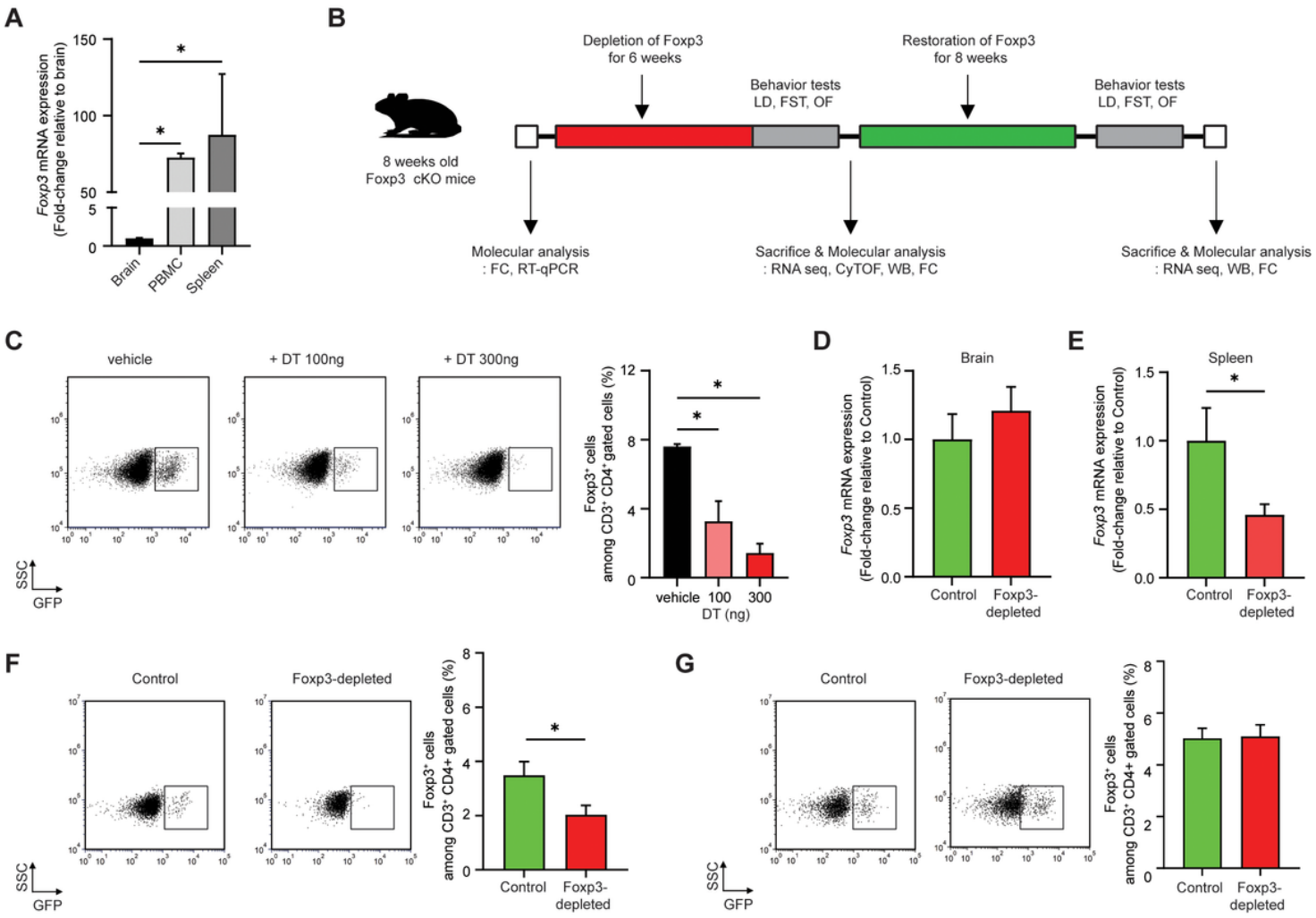

Figure 1

Transient depletion of Foxp3 expression followed by DT treatment in Foxp3 cKO mice

(A) A bar graph showing Foxp3 mRNA expression in brain, PBMC and spleen. Statistical analyses were performed using one-way ANOVA, followed by Tukey's post hoc analysis (*p<0.05, compare to Foxp3 mRNA expression in brain, n = 3-6 mice for each group. (B) Experimental outline (FC, flow cytometry; RNA seq, RNA sequencing; CyTOF, cytometry by time of flight; WB, western blot; LD, light and dark box; FST, Forced swimming test; OF, open field). (C) Representative flow cytometry analysis of GFP expression by gated $CD3^+CD4^+$ cells (left panel). Bi-exponential scale used for representative flow cytometry. A bar graph showing percentage of $Foxp3^+$ cells among $CD3^+CD4^+$ cells in PBMC of Foxp3 cKO mice followed by treatment of different dose of DT (right panel). Statistical analyses were performed using one-way ANOVA, followed by Tukey's post hoc analysis (*p<0.05, compare to control group, n = 3-4 mice for each group). (D-E) Foxp3 mRNA expression (D) in brain and (E) in spleen followed by DT treatment in Foxp3 cKO mice. Bar graphs showing relative quantification of Foxp3 mRNA expression in Foxp3-depleted and

age matched control mice. (F-G) Representative flow cytometry analysis of GFP expression by gated $CD3^+CD4^+$ cells from PBMC in (F) Foxp3-depleted mice and in (G) Foxp3-restored mice compared to age matched control mice. Bar graphs showing percentage of $Foxp3^+$ cells among $CD3^+CD4^+$ cells. Bi-exponential scale used for representative flow cytometry. Statistical analyses were performed using t-test (*p<0.05, compared to age matched control mice, n = 5-7 mice for each group). Data are expressed as the means ± SEM.

Figure 2

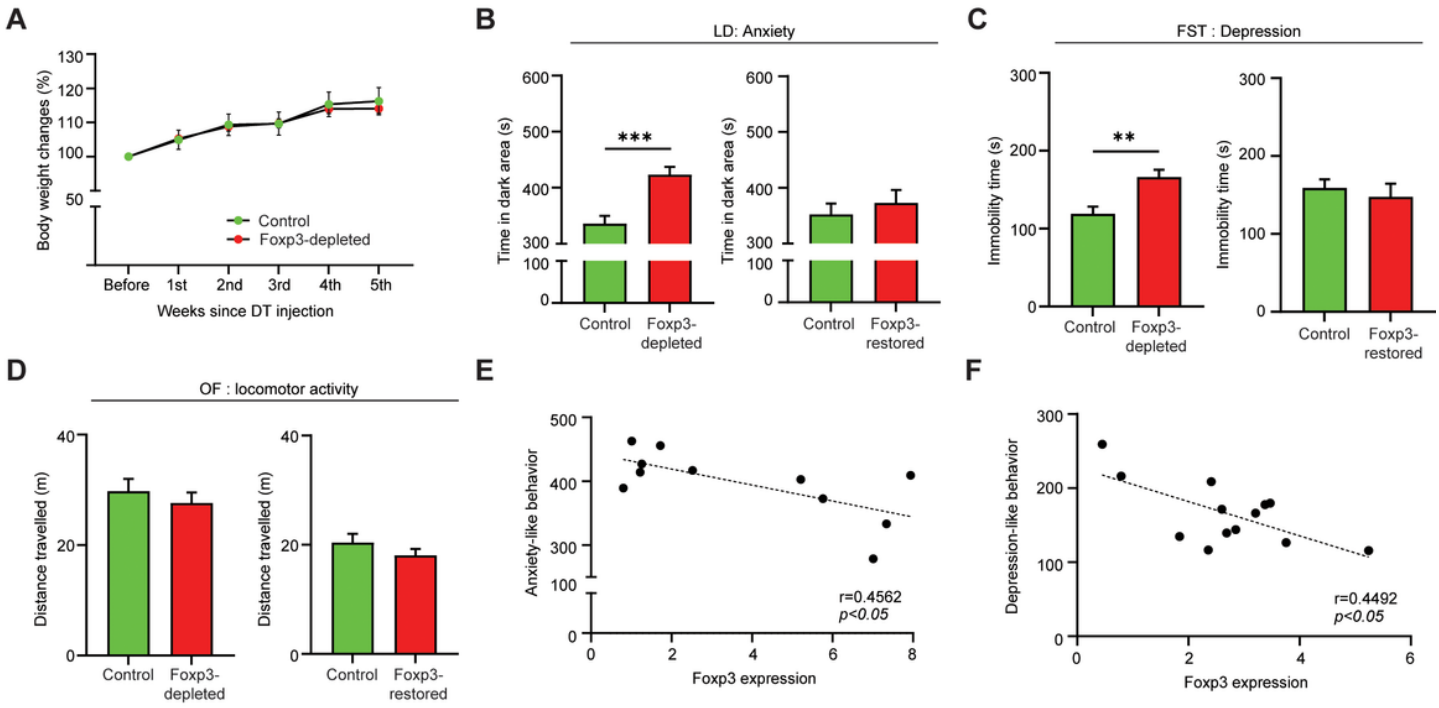

Figure 2

Transient depression and anxiety like-behaviors mediated by depletion of Foxp3 expression in Foxp3 cKO mice

(A) Body weight changes in Foxp3 cKO mice followed by vehicle or DT treatment. (B) Bar graphs showing time spent in dark compartment in Foxp3-depleted and Foxp3-restored mice compared to age matched control mice as a measure of anxious-like behavior in LD. (C) Bar graphs showing total immobility time compartment in Foxp3-depleted and Foxp3-restored mice compared to age matched control mice as measure of depression-like behavior in FST. (D) Bar graphs showing total distance traveled throughout the apparatus compartment in Foxp3-depleted and Foxp3-restored mice compared to age matched control mice as measure of locomotion activity in OF. (E-F) Scatter plots representing the correlation between Foxp3 expression and (E) anxiety-like behavior and (F) depression-like behavior in Foxp3-depleted and Foxp3 restored mice. Statistical analyses were performed using t-test (**p < 0.01 ***p< 0.001, compared to age matched control mice, n = 10-15 mice for each group). Data are expressed as the means ± SEM.

Figure 3

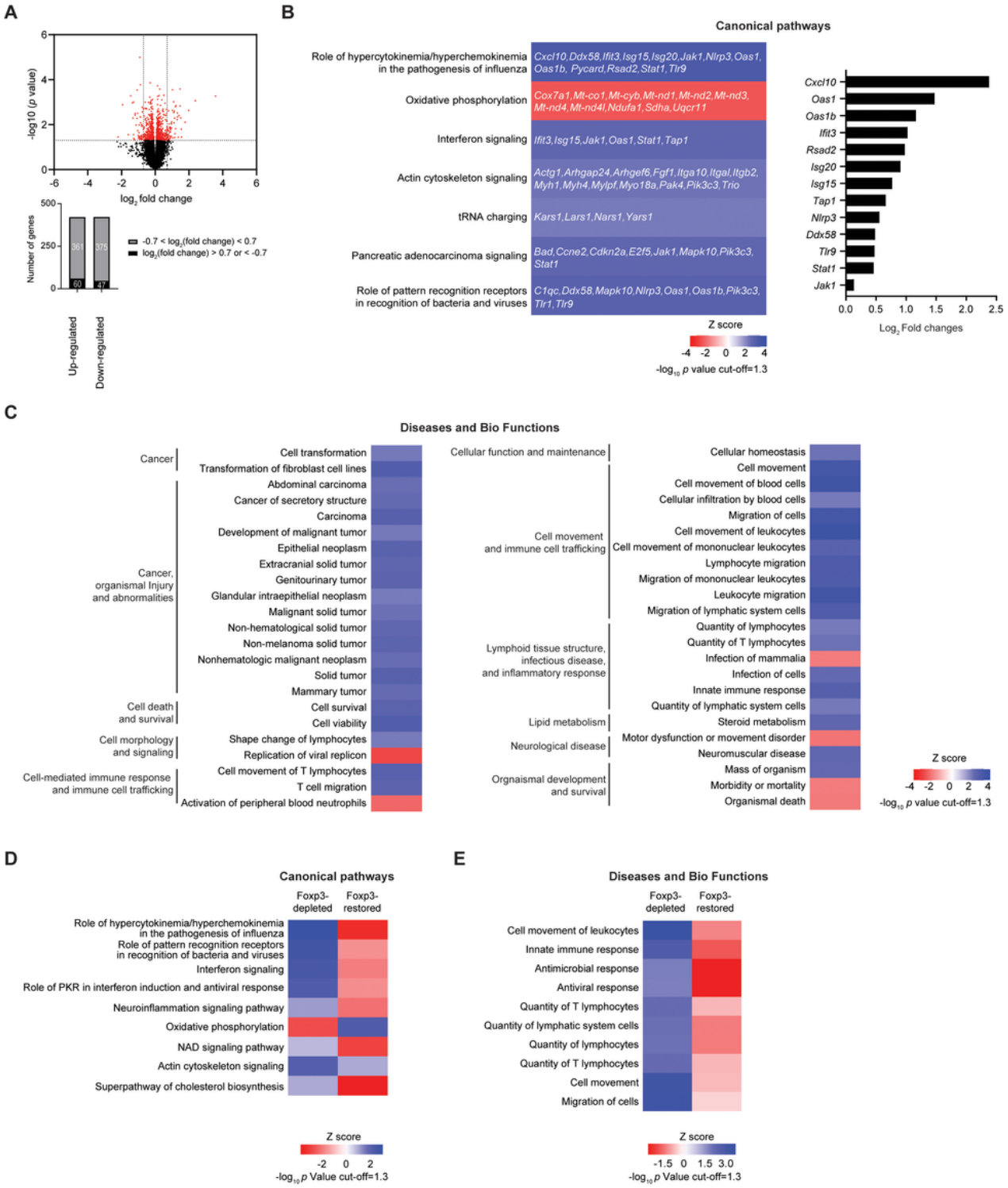

Figure 3

Alteration of differentially gene expression profiles mediated by Foxp3 expression in hippocampal formation of Foxp3 cKO mice

(A-C) Prediction of biological functions and canonical pathways which are activated or inactivated in Foxp3-depleted mice compare with age matched control mice according to ingenuity pathway analysis.

(A) A volcano plot (upper panel). The x-axis represents the $\log_2$ conversion of the fold change (FC) values, and the y-axis represents the corrected significance level after base $\log_{10}$ conversion (*p* value). Red dots in the volcano plot indicate all DEGs that were found to differ significantly (*p <0.05). The number of significant DEGs (bottom panel). The black bar represents the number of genes with an absolute value of $\log_2$ FC greater than 0.7 and the gray bar represents the number of genes with an absolute value of $\log_2$ FC less than 0.7. (B) A heatmap representing canonical pathways analysis (left panel). Activated canonical pathway (blue bar) and inhibited canonical pathway (red bar) were identified by applying absolute value of Z score > 2. FC value of selected DEGs which are related to top 3 canonical pathways (right panel). (C) Heatmaps representing diseases and biological functions analysis. Activated canonical pathway (blue bar) and inhibited canonical pathway (red bar) were identified by applying absolute value of Z score > 2. (D-E) Comparison analysis of (D) canonical pathways and (E) diseases/bio functions between Foxp3-depleted and Foxp3-restored mice. Z-scores were used to predict activation or inhibition. Statistical analyses were performed using the Wald test (*p < 0.05, compare to age matched control mice, n = 6-9 mice for each group).

Figure 4

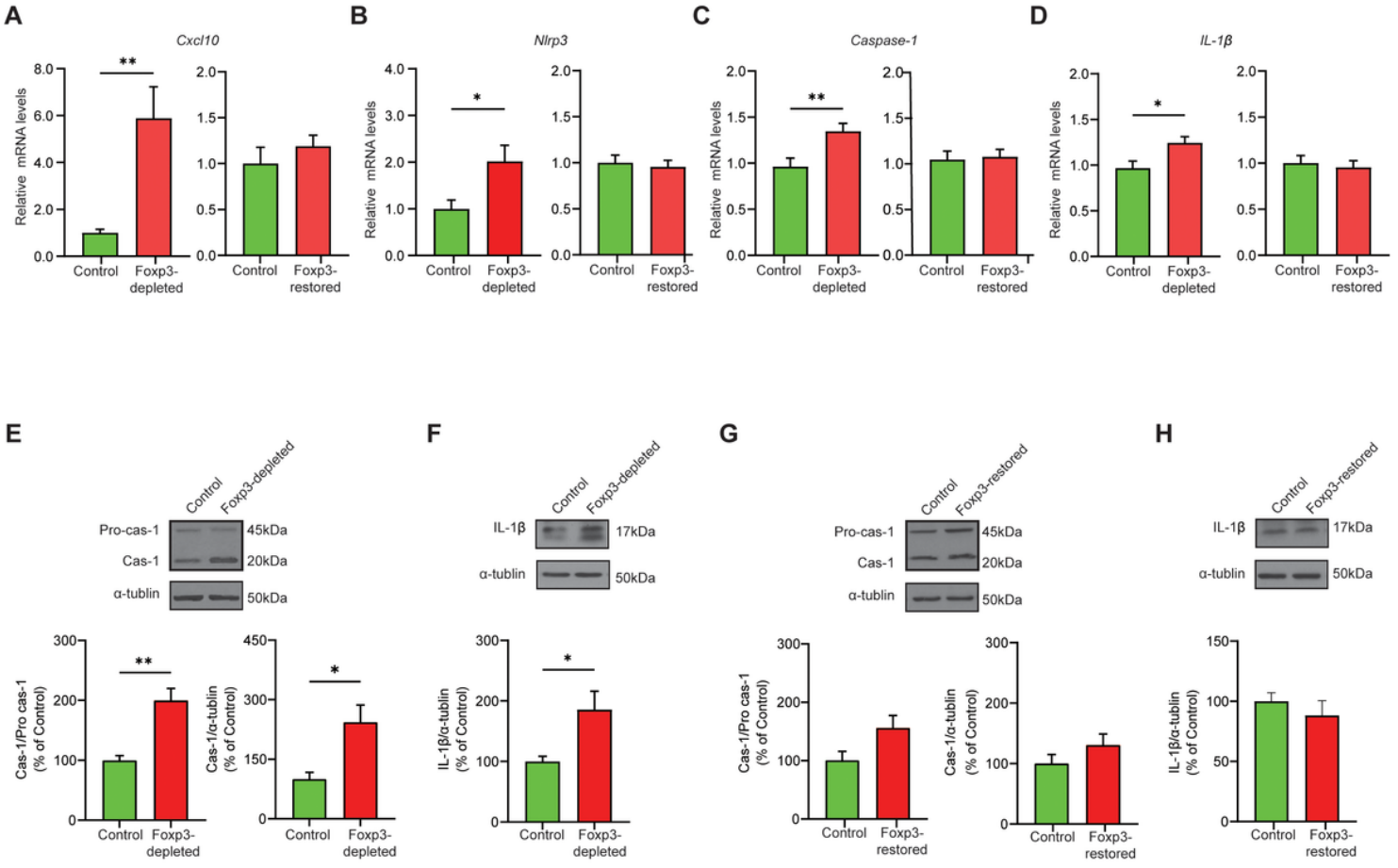

Figure 4

Transient activation of inflammasome signaling pathway in hippocampal formation of Foxp3 cKO mice

(A-D) The mRNA expression of Cxcl10, Caspase-1, Nlrp3 and IL-1β in hippocampal formation of Foxp3-depleted mice (left panels) and Foxp3-restored mice (right panels). Bar graphs showing relative quantification of Cxcl10 (A), Caspase-1 (B), Nlrp3 (C) and IL-1β (D) levels normalized Hprt. (E-H) Representative western blot of pro-casepase-1, caspase-1 and IL-1β in Foxp3-depleted (E and F) and Foxp3-restored mice (G and H). Bar graphs showing relative quantification of cleaved caspase-1, ratio caspase-1/pro-caspase-1 (E and G) and IL-1β (F and H) levels normalized α-tubulin. Statistical analyses were performed using t-test (*$p < 0.05$, **$p < 0.01$, compared to age matched control mice, n = 4-8 mice for each group). Data are expressed as the means ± SEM.

Figure 5

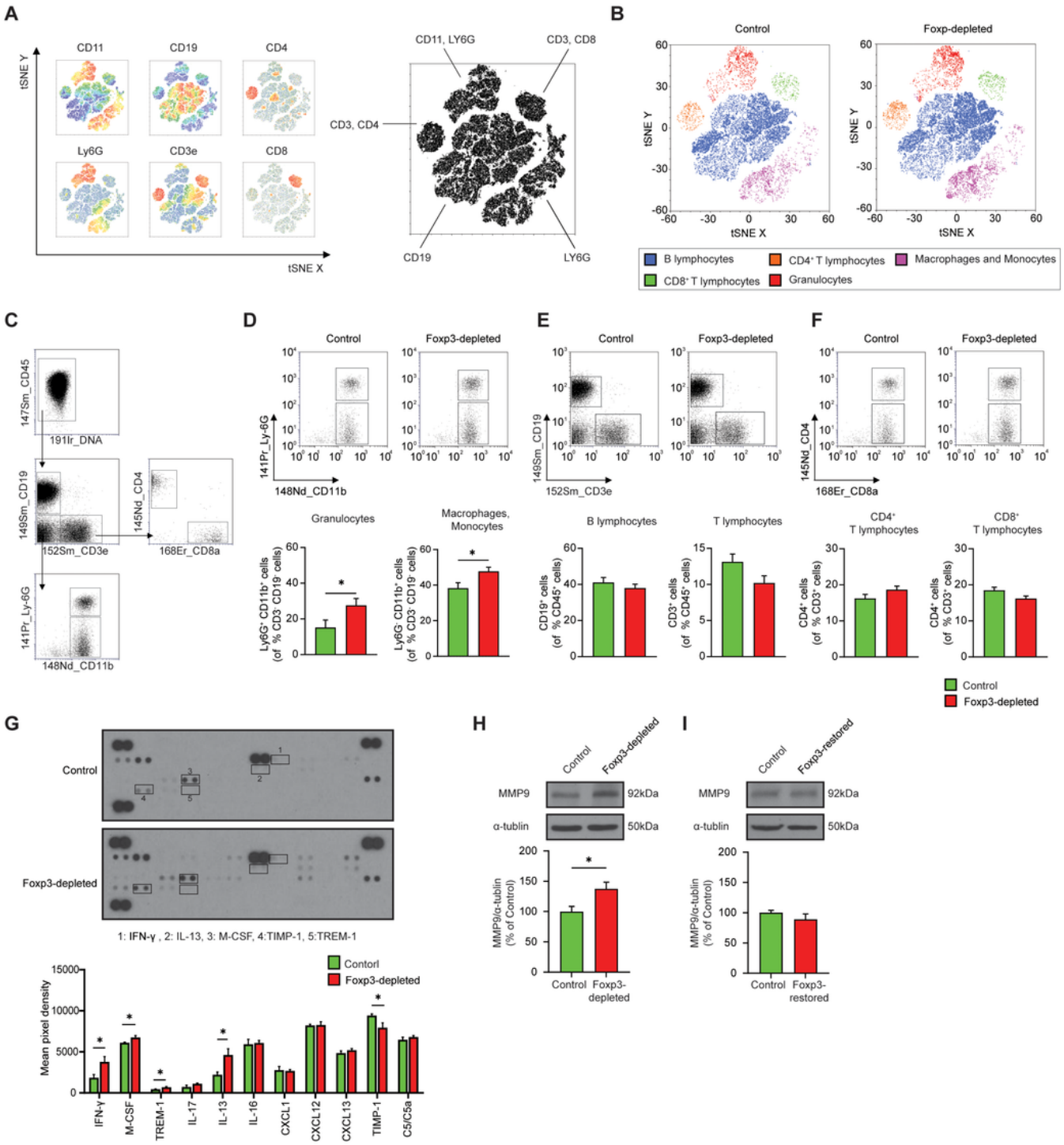

Figure 5

Characterization of peripheral immune cell population and transient MMP-9 expression mediated by Foxp3 expression in Foxp3 cKO mice

(A-B) t-SNE plots generated from the CD45^{+} immune cell populations stained by CyTOF in PBMC of Foxp3-depleted mice. (A) Heat maps showing expression of selected markers by immune cells clustered

using t-SNE analysis. (B) t-SNE plots separated into 5 broad groups of immune cells (B lymphocytes, $CD4^+$ T lymphocytes, $CD8^+$ T lymphocytes, macrophages/monocytes and granulocytes) in Foxp3-depleted mice compared to age matched control mice. The main cell populations are shown by the indicated color profile. (C) Gating strategy for CyTOF analysis. (D-F) Representative CyTOF scatter plots (upper panel) and quantification of lymphocyte subpopulation (bottom panel). Bar graphs showing percentage of $CD11b^+$LY-$6G^+$ (D), $CD11b^+$LY-$6G^-$ (D), $CD3e^-$ $CD19^+$ (E, left panel), $CD3e^+CD19^-$ (E, right panel), $CD3e^+CD4^+$ (F, left panel) and $CD3e^+CD8^+$ (F, right panel) cells in Foxp3 depleted mice compared to age matched control mice. Scales are shown in bi-exponential scale. (G) Representative blot image of the cytokine array data in Foxp3-depleted and age matched control mice (upper panel). Bar graphs showing quantification of mean pixel density of cytokines and chemokines among 40 cytokines (bottom panel). The mean pixel densities of each spot were normalized by reference spots. (H-I) Representative western blot of MMP-9 (upper panel). Bar graphs (bottom panel) showing relative quantification of MMP-9 level normalized α-tubulin in hippocampal formation of Foxp3-depleted mice (H) and Foxp3-restored mice (I). Statistical analyses were performed using t-test. (*$p < 0.05$, compare to age matched control mice, n =6-8 mice for each group). Data are expressed as the means ± SEM.

Figure 6

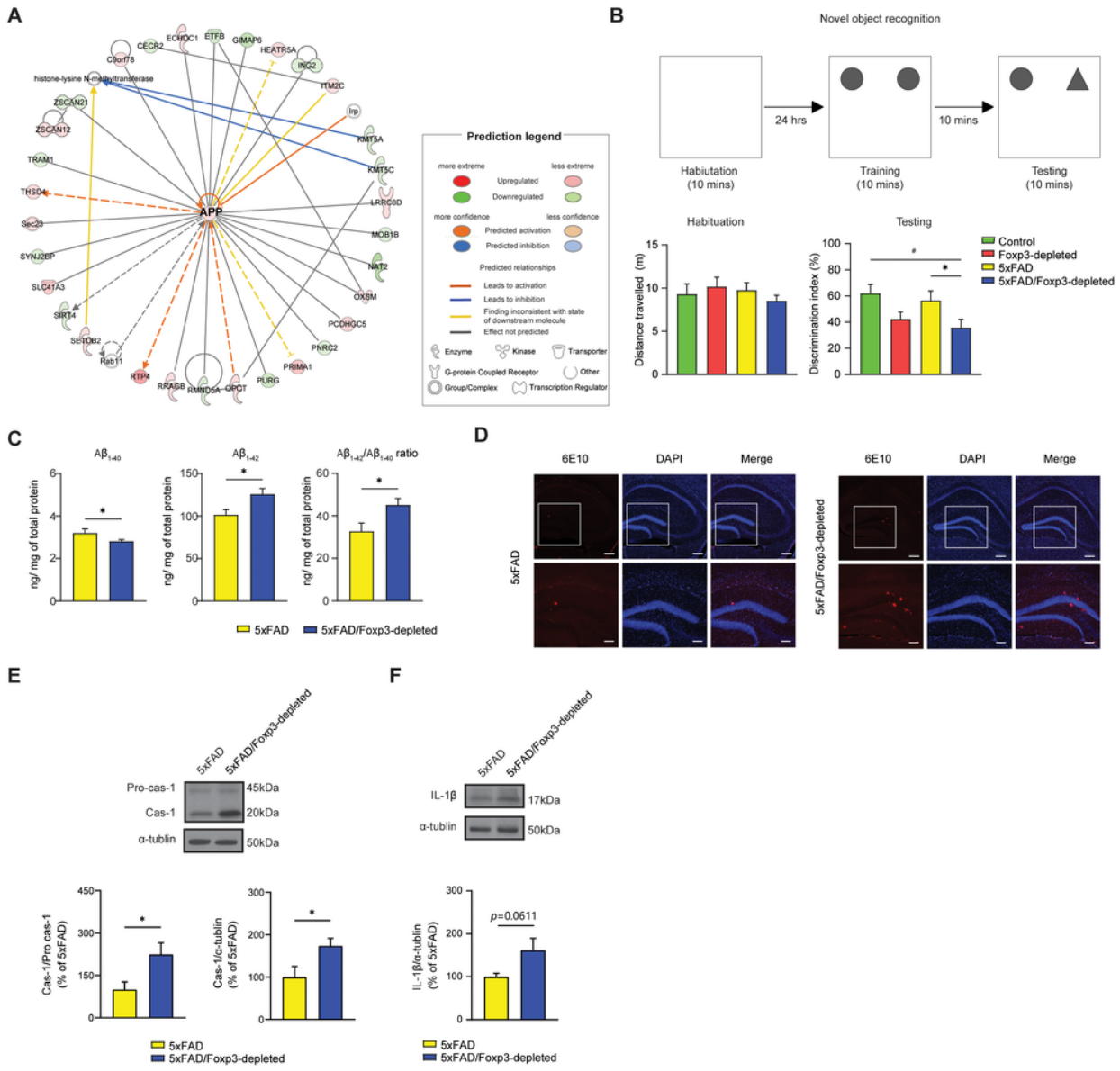

Figure 6

Cognitive decline, accumulation of Aβ and inflammasome activation mediated by depletion of Foxp3 expression in 5xFAD/Foxp3-depleted mice

(A) Functional gene networks identified using IPA analysis in hippocampal formation of Foxp3-depleted mice. Predict legend indicates each node's relationship from machine-based learning. (B) Scheme illustration of novel object recognition test (upper panel). Bar graphs showing locomotion activity as measure of total distance traveled in habituation session (bottom, left panel) and discrimination index as measure of percent time spend with the novel object in testing session (bottom, right panel). (C) The level of soluble $A\beta_{1-40}$, $A\beta_{1-42}$ in the hippocampal of 5xFAD/Foxp3-depleted mice. Bar graphs showing quantification of $A\beta_{1-40}$, $A\beta_{1-42}$ and the ratio of $A\beta_{1-42}/A\beta_{1-40}$ compared to age matched 5xFAD mice. (D)

Representative immunohistochemical images showing 6E10-labeling Aβ plaques (red) and DAPI (blue) nuclei in the dentate gyrus of 5xFAD/Foxp3- depleted and age matched 5xFAD mice. The outlined with a white box in upper panel is magnified in bottom panel. The scale bars indicate 200 μm (low-scaled panel) and 100 μm (magnified panel). (E-F) Representative western blot of pro-casepase-1, caspase-1 and IL-1β in 5xFAD Foxp3-depleted mice. Bar graphs showing relative quantification of cleaved caspase-1 (E, left panel), ratio of caspase-1/pro-caspase-1 (E, right panel) and quantification of IL-1β (F) levels normalized α-tubulin. Data are expressed as the means ± SEM. Statistical analyses were performed using t-test or two-way ANOVA, followed by Tukey's post hoc analysis. (*$p < 0.05$, compare to age matched 5xFAD control mice, $^{\#}p < 0.05$, compare to age matched Foxp3 control mice n = 6-10 mice for each group)

Supplementary Files

This is a list of supplementary files associated with this preprint. Click to download.

- suppleFig1.tif